EXPERIMENTAL INVESTIGATION OF CAVITATION SIGNATURES IN AN AUTOMOTIVE TORQUE CONVERTER USING A MICROWAVE TELEMETRY TECHNIQUE

C. L. Anderson, L. Zeng, P. O. Sweger, A. Narain
Dep't. of Mechanical Engineering-Engineering Mechanics
Michigan Technological University, Houghton, MI 49931

J. R. Blough
Keweenaw Research Center
Houghton, MI 49931

ABSTRACT

A unique experimental investigation of cavitation signatures in an automotive torque converter under stall conditions is reported. A quantitative criteria is proposed for predicting early and advanced cavitation in terms of suitable non-dimensional pump speeds. The dimensionless pump speed that marks early cavitation is obtained by relating this parameter to appearance of charge-pressure dependent pressure fluctuations in the differential pressure transducer readings. The differential pressure transducers were mounted at well defined locations in the pump passage of a torque converter. The data were transmitted by a wireless telemetry system mounted on the pump housing. Data were received and processed by a ground-based data acquisition system. Automatic transmission fluid (ATF) exhibited cavitation for charge pressures of 70-130 psi and pump speeds of 1000-2250 rpm. Advanced cavitation was marked by operating conditions that exhibited a 2% or more torque-degradation from the converter's non-cavitating performance.

For a given family of torque-converter designs and a given transmission fluid, the proposed non-dimensional pump- speed criteria are capable of marking early and advanced stages of cavitation for a range of torque-converter sizes and a range of charge pressures in the torque-converter.

INTRODUCTION

The automotive torque converter (Maddock 1991) is a complex turbo machine that consists of three elements: a pump, a turbine, and a stator. It is used in the automatic transmission of a vehicle to transfer power from the engine to the transmission gearing during driving and to effectively unload the engine during idle. It multiplies engine torque during vehicle launch and dampens engine torsional vibration and inertial transients.

Power is transmitted from the engine to the driveline by alterations in the angular momentum of a stream of fluid that constantly circulates between the converter elements. Petroleum based automatic transmission fluid (ATF) is used as the working medium. A typical automotive torque converter cross section and flow path are shown on Fig. 1. The converter pump is attached to the engine crankshaft and rotates at engine speed.

Fluid flowing between the pump blades is expelled from the pump outlet and immediately enters the turbine. The exiting fluid possesses a high velocity in the direction of pump rotation and consequently a high angular momentum. The turbine blades guide the fluid inward and direct it opposite of pump rotation, causing a large change in its angular momentum. This results in a torque on the turbine and which is transmitted to the transmission gearing by the turbine shaft. Upon leaving the turbine, the fluid has a relatively low or even negative (opposite pump rotation) tangential velocity and angular momentum. The stator receives this fluid and accelerates it back in the direction of pump rotation. Once again, the accompanying change in angular momentum produces torque on the stator and this

torque is resisted by a non-rotating shaft built into the transmission housing. Finally, fluid reenters the pump, carrying with it momentum in the direction of pump rotation. As a consequence of the flow vectoring by the stator, pump torque is less than turbine torque (torque is "multiplied"), and this difference is exactly equal to the stator torque.

In all three elements pressure forces between the blades and the working fluid accomplish the change in angular momentum. The blades bend the streamlines of the flow, and this action elevates the static pressure on the leading (pressure) side of the blade while dropping pressure on the trailing (suction) side. The total element torque is the product of the pressure difference across the blade and the radius from the shaft center line, integrated over the blade surfaces. When torque into the converter pump increases, as when the engine throttle is opened, leading and trailing side pressures are forced higher and lower, respectively. At some level of input torque, the pressure on the suction side of the stator blades will drop below the vapor pressure of the fluid, allowing the fluid to cavitate.

NOMENCLATURE

Ca'	fluctuating cavitation number
D	diameter of pump
f	frequency
PS	power summation
K	K factor
MSP	mean square pressure
p′	fluctuating pressure
p_c	charge pressure
p_e	exit pressure
ρ	density of ATF
Ω	pump speed, rad/s
$\tilde{\Omega}_p$	non-dimensional pump speed
μ	viscosity
T_p	pump torque
Φ	local flow variable

GENERAL CONSIDERATIONS

Torque Converter Cavitation

Cavitation is expected at any location in a flowing liquid where the local pressure is at or below vapor pressure of the liquid (vapor pressure of a significant component of a liquid in case of a multi- component liquid such as ATF) at the local temperature. Local vaporization of the liquid at any nucleation site then causes development of a vapor-filled bubble or cavity in the flow. As the cavities move into regions where pressure is higher than the local vapor pressure, a combination of compression and rapid condensation of the vapor in the cavity causes the collapse of the cavity. At the point of disappearance of the cavity, the pressure momentarily raises to a high value, leading to subsequent pressure fluctuations. The amount of cavitation depends on the mean absolute pressure levels in the flow, and in this investigation a representative value is taken to be the torque converter charge pressure. This dependence distinguishes cavitation induced pressure fluctuations in an incompressible flow from those that arise from rotating

machinery or turbulence induced fluctuations which, necessarily, are independent of the mean absolute pressure levels.

Cavitation is suppressed by pressurizing the torque converter torus with ATF from the transmission's hydraulic control system. This pressure, commonly termed converter charge pressure, is superimposed on the pressure field of the turbomachine and consequently raises the torque at which cavitation will occur.

Cavitation is to be avoided in automotive torque converters for two reasons. First, noise caused by even mild cavitation is noticeable in the passenger compartment of most vehicles and is of such a nature that it can cause customer complaints. The noise can be audible at light throttle, low charge pressure conditions, when there is little engine noise to mask it, or during heavy throttle acceleration. Secondly, the disruption of the converter's normal speed-torque characteristics allows the engine to run in regions of its own speed-torque envelope where it is not expected to operate. This is most often noticed as inconsistent vehicle performance or excessive transmission temperature.

Since the effects of cavitation are also important in other fluid machinery, there is a large amount of literature which deal with the broad subject of cavitation and its effects on walls (Knapp 1970, Rheingas 1961, etc.). There are also a large number of fundamental studies which deal with bubble or bubble population dynamics in cavitation (e.g. Plesset and Prosperetti 1977, Ceccio and Brennen 1992, Kumar and Brennen 1993, etc.). This paper's study of cavitation signatures in an automotive torque-converter is, however, more in the spirit of identification of cavitation in pumps through suitable cavitation numbers and net positive suction head (NPSH) values. While we are not aware of cavitation studies for a torque converter, some relevant cavitation studies for pumps are: Franz et al. (1990), Ardizzon and Pavesi (1994), Hashimoto et al. (1997), etc.

Detection of Cavitation

Laboratory evaluation of cavitation in automotive torque converters has generally been limited to the determination of the pump torque at which the converter deviates from the ideal parabolic pump speed vs. pump torque curve. This curve is usually obtained at stall condition and at constant charge pressure and temperature. The results have not been completely satisfying because the large net power input to the converter forces rapid heating. This creates pressure, torque and speed transients which exceed the typical test equipment's capabilities to detect cavitation induced variations. Noise evaluation has been even less successful because background noise in the test cell overwhelms anything generated by the converter.

The approach taken in this work is to associate pressure fluctuations in the working fluid of the converter with the onset and development of cavitation. If the point of a cavity collapse is close to a boundary wall the resulting pressure spikes can first be recorded by a pressure transducer before an effect on the mean values of the flow variables (torque) can be detected.

A zone in the flow field that includes the formation, maintenance, and disappearance locations of the cavities is called a cavitation zone. Converters operating under low torques and high charge pressures will not cavitate and would have no cavitation zones. Conversely, high input torques and low charge pressures will produce large, strong cavitation zones (associated with the size and number of the cavities). These conditions produce a measurable departure from the non-cavitating speed-torque characteristic. Between these two conditions there is a range in which cavitation zones will be formed but will not be of sufficient influence on the flow to produce an identifiable deterioration of the speed-torque characteristic. For the purposes of this study, conditions which induce a 2% loss of pump torque at a given pump speed will be termed *advanced cavitation*. Conditions that exhibit abnormal pressure fluctuations but do not support a 2% torque degradation will be termed *early cavitation*.

Telemetry

The pressure measurements were acquired from the rotating torque converter using a wireless telemetry technique (Zeng 2000). A 2.5 GHz carrier wave was used to transmit the transducer information. The technique typically uses conventional transducers and a microwave transmitter on the moving part. The evolution of the signal is shown in Fig. 2.

A voltage-to-frequency conversion is performed on the output of the transducer. The 0-100 kHz V/F converter is very stable and can be operated across a wide range of temperature. The resulting signal is then used to modulate a voltage-controlled oscillator (2.5 GHz). The transducer information is thus superimposed on the carrier wave and is transmitted from the moving part using a dipole antenna milled into the transmitters housing.

The signal is received by a pair of stationary antennas, down converted and processed by an external receiver to reconstruct the original frequency modulation. An analog frequency-to-voltage conversion is performed at the output of the receiver to reconstruct the transducer signal. This final F/V conversion typically requires a low-pass filter with a cut-off frequency of three kHz.

The wavelength of the transmitted signal is small enough that it can easily propagate through the open spaces inside rotating and reciprocating machinery, such as engines and transmissions. The 2.5 GHz carrier wave transmitted from the moving part fills either the bell housing or, in the case of this investigation, the laboratory test fixture with the signal. The microwave transmitter and the battery packs that power the electronics are shown mounted on the pump in Fig. 3.

CAVITATION SIGNATURES

At a specified transducer location, a transducer's pressure response, *p(t)* is composed of a steady pressure component and a fluctuating pressure component, $p'(t)$, as

$$p(t) = \overline{p} + p'(t) \tag{1}$$

We expected to find cavitation signatures in the fluctuating pressure signal, p'. The fluctuating pressure p' was obtained with the help of a differential pressure transducer whose reference tube was routed back to the transducer's sensing location as shown in Fig. 4. The diameter and the length of the reference tube was chosen to ensure that the fluctuating component p' acting at the reference tube opening was significantly damped by the time this signal reached the reference side of the diaphragm. This fact was experimentally established (Zeng 2000). In this configuration $\overline{p} + p'$ acted on the measurement side of the transducer's diaphragm and $\overline{p}$ on its reference side. Thus the voltage signal obtained from the 10 psi differential pressure transducers truly represented p'.

In principle one might expect to characterize cavitation signatures (the strength of the fluctuating pressure) using a *mean square pressure* MSP, where

$$MSP = \left(\int_o^T p'^2 dt \right) / T, \tag{2}$$

is a representative square amplitude nearly independent of the duration T of the fluctuating pressure, p'. However, for these experiments, it is preferable to use a frequency-filtered mean square pressure which retains only a frequency range $f_1 \le f \le f_M$ of the signal p' that is relevant to cavitation. To define frequency-filtered MSP, first

we converted the time domain signal p' over $0 \le t \le T$ to the frequency domain by obtaining a discretized version of the Fourier Transform P(f),

$$P(f) = \frac{1}{T}\int_0^T p'(t) e^{-i2\pi f t} dt. \tag{3}$$

The P(f) values were replaced by $P_i(f)$ values which are the Fast Fourier Transform of pressure signals p_i' for $1 \le i \le N$ obtained by dividing the original p' signal of duration T (here T=2.3 seconds) into N equal records (here N = 20) of duration T/N. Then, in order to get a clearer spectrum by reduction of random noise, an ensemble averaged power EAP in the frequency domain was defined as

$$EAP(f) = \frac{\left(\sum_{i=i}^{N} |P_i(f)|^2 \right)}{N}. \tag{4}$$

We wanted the filtered mean square pressure to be a measure of signal energy over a resolvable frequency range $f_1 \le f \le f_M$ such that its value is independent of record duration T and the number N of sub-records obtained from the original signal record of duration T. For the above reasons, *power summation* PS is defined as

$$PS = (T/N)\int_{f_1}^{f_M} EAP(f) df \cong \sum_{i=1}^{M} EAP(f_i), \tag{5}$$

where M is the number of frequency data points of EAP for a given scan rate S (here S is 20,000 samples per second), duration T, and number of divisions N of the original record length T. Typically the highest frequency f_M is less than $f_{Nyquist} = S/2$ and $f_1 > N/T$. A restriction on f_M was imposed by a *low pass filter* imbedded in the receiver of the telemetry system depicted in Fig. 2. Both theoretically, and computationally, it was established that PS defined in Eqn. 5 is reasonably independent of scan rate, record length T, and number of divisions N of the original record length T. It should be noted that both the mean square pressures MSP and PS have SI units of Pa^2 and USC units of psi^2.

For stall condition (fixed turbine) and steadily rotating pump (at a rotation rate Ω), any time-averaged local flow variable Φ (such as MSP, PS, etc.) at a point inside a torque converter would depend on quantities that typically determine the solution of the torque converter's boundary value problem. Therefore, for cavitating flows, one must add charge pressure p_c (pressure at the inlet of the torque converter) and vapor pressure p_v (at a representative flow temperature) to the list of parameters that typically determine the flow field in non-cavitating flows. It is easy to see that the variable Φ will depend on the shape and size (size is determined by pump diameter D) of the torque converter, location of the point in the flow field where Φ is measured, pump speed Ω, charge pressure p_c, vapor pressure p_v, representative mean values of fluid density ρ and viscosity μ at a representative temperature, and pressure difference $(p_c - p_e)$, or through-put oil flow rate Q, between the inlet and the exit of the torque converter. As an approximation, it can be assumed that the pressure difference $p_c - p_e$ is primarily determined by the pump speed Ω and only secondarily determined by the through-put flow rate Q. It can be further assumed that, at reasonably fast pump speeds, the Reynolds number $(\rho D^2 \Omega)/\mu$ is large, so effects of viscosity μ are negligible (as is the case for centrifugal pumps under fully rough turbulent flow conditions). Therefore, for a given family of torque converters, a given fluid (ATF), and a given transducer location, the more significant variables affecting Φ are given by the assumption:

$$\Phi \cong function(D, \Omega, \rho, p_c). \tag{6}$$

The dimensionless form of Eqn. 6, for $\Phi = \sqrt{PS},$ is easily obtained (see Π-Theorem in Munson et al. 1998) and is given by:

$$Ca' \equiv function\left(\tilde{\Omega}_p\right), \tag{7}$$

where Ca' is a nondimensional fluctuating pressure which we refer to as the *fluctuating cavitation number* and is defined as

$$Ca' = \left(\sqrt{PS}\right) \Big/ \left(\frac{1}{2}\rho(D\Omega)^2\right), \tag{8}$$

and $\tilde{\Omega}_p$ is dimensionless pump speed defined as

$$\tilde{\Omega}_p \equiv \left(D\tilde{\Omega}\right) \Big/ \left(\sqrt{p_c/\rho}\right) \tag{9}$$

It should be recognized that at small values of pump speeds Ω, experimentally obtained Ca' values may not exactly follow Eqn. 7 as the Reynolds number $\rho D^2\Omega/\mu$, or an equivalent viscosity parameter such as $D\sqrt{\rho p_c/\mu}$, should be included in addition to $\tilde{\Omega}_P$ in the argument list of Eqn. 7.

EXPERIMENTAL PROCEDURE AND RESULTS

Test Apparatus

The torque converter tests were performed in a laboratory fixture. The fixture housed the converter and supported both the input and output shafts. A separate hydraulic unit supplied ATF to the fixture and provided control over flow rate, temperature and charge pressure. Inlet pressure (charge pressure), inlet temperature, outlet temperature, and outlet pressure for the converter were measured.

All of the data reported in this investigation were acquired for the stall condition. This condition simulates the initial stages of vehicle launch, a condition at which cavitiation is sometimes observed. During stall conditions the toroidal flow through the blade elements is the greatest and the separation region on the suction side of the stator blade is expected to be at its lowest pressure.

The transducers were installed behind static pressure taps in the pump. It was expected that cavities would form on the suction side of the stator blade and move with the toroidal flow into the pump. The cavities were expected to collapse somewhere in the pump passage as the pressure of the ATF increased. Static pressure taps were located at five different stations as shown in Fig. 5. The taps were located along the passage center line. The pressure taps are shown schematically in Fig. 5 to be located in the same pump passage. However in the actual test converter the pressure taps were located in adjacent passages.

Test Matrix and Data Acquisition

In this study, pump speed and charge pressure were varied over ranges that were believed to adequately cover conditions that might be encountered in actual operation. Pump speed was varied from 500 rpm to 3000 rpm in increments of 250 rpm. Charge pressure was varied from 70 psi to 130 psi in increments of 10 psi. At all test conditions the inlet temperature was held constant at 80 degrees C and outlet temperature would settle to an equilibrium temperature based on the amount of power input to the oil. Data was acquired at steady state conditions as long as the outlet temperature was below 120 degrees C. At higher pump speeds, data acquisition was initiated as soon as outlet temperature exceeded 120 degrees C in order to protect the electronics and batteries.

Five single-channel transmitters were mounted on the pump for the pressure measurements. The data was transmitted simultaneously at slightly different carrier frequencies. Each transmitter was paired with its own receiver which down converted the signal and reconstructed the transducer output. Data was acquired with a PC-based data acquisition system.

Results and Discussion. Various $p'(t)$ signals at the above specified pressure transducer locations were obtained by converting the transducer's raw real time voltage signal through proper calibrations (Zeng 2000). At a pump speed of 1750 rpm, we show in Fig. 6 representative p' signals from the transducer at Station 25 for charge pressure p_c values of 130 psi and 70 psi respectively.

As stated earlier, the fluctuating pressure p' in these two figures could be due to three reasons: (i) flow fluctuations arising from mechanical forcing functions associated with shaft rotation, various blade passages, etc.; (ii) flow turbulence; and (iii) the collapse of vapor cavities typically associated with cavitation. Among these three phenomena only cavitation is strongly influenced by charge pressure. Fig. 6 clearly indicates the increasing trend of the fluctuating pressure when the charge pressure was reduced from 130 psi to 70 psi. This is indicative of cavitation. Such cavitation signatures would now be quantified and related to the flow variables through proper processing of the fluctuating pressure p' data.

For the signals in Fig. 6, we obtained $|P(f)|$ defined in Eqn. 3 and EAP(f) defined in Eqn. 4. These are respectively shown in Fig. 7 and Fig. 8. The EAP(f) values for each of the charge pressures tested are included in Fig. 8. An increase in EAP(f) with decreasing charge pressure can be observed in Fig. 8. This trend is what one would expect to see in a cavitation signature as charge pressure decreased. The signature has a fairly broad spectral distribution. The roll-off in EAP(f) above 3000 Hz is due to the effects of the low-pass filter in the microwave receiver.

For each charge pressure and pump speed tested, the EAP (f) values were then summed from f_1 ~ 0 Hz and f_M = 4000 Hz to obtain PS through its definition in Eqn. 5. Resulting values of PS as a function of pump speed and charge pressure are shown in Fig. 9. The charge pressure dependency begins to be clear above line MB. We refer to this as early cavitation because, as we see later, there is no noticeable effect on the pump performance measured at the dynamometer. Yet, from the *in situ* measurements, we see a noticeable onset of charge pressure dependency in the region above line MB.

Next, PS values obtained for Fig. 9 are used to obtain the *fluctuating cavitation number* Ca' in Eqn. 8 and the results are plotted, with the help of the non-dimensional pump speed $\tilde{\Omega}_p$, in the form suggested by Eqn. 7. This results in a relationship of the type shown in Fig. 10.

Clearly, in Fig. 10, there is only an approximate single curve - which appears to be linear - of the type suggested by Eqn. 7 in the range $1.32 < \tilde{\Omega}_p < 1.76$. All the data in this region do not collapse perfectly to a single curve because of experimental errors and perhaps because we neglected the non-dimensional parameter that represents $p_c - p_e$ to account for variations in throughput flows. At lower pump speeds, effects of non-dimensional viscosity, and, at higher pump speeds, effects of fluid property variations with time and temperature are expected to enhance departure from the primary relationship indicated by Eqn. 7. Despite this, considering the enormous complexity of the flows, Fig. 10 justifies use of Eqn. 7 for the sought after cavitation signatures.

The charge pressure dependency approximately began above line MB in Fig. 9. When these points were transformed and superposed on power summation curves of Fig. 10, line MB of Fig. 9 transformed to a vertical line MB $\left(\tilde{\Omega}_p \approx 1.32\right)$and the "above MB zone" of Fig. 9 mapped to $\tilde{\Omega}_p > 1.32$. This implies that the proposed early cavitation criteria of $\tilde{\Omega}_p \approx 1.32$ is reasonable.

To define an advanced cavitation regime, we look at the pump's "torque versus pump-speed" performance with the help of stall condition "K factor" values, where $K \equiv \Omega / \sqrt{T_p}$. For non-cavitating stall situations, K-factor is known to be a constant (Maddock 1991). The non-cavitating value, for the torque converter used in the test facility, is 220.5 and is shown on the torque curve in Fig. 11. A 2% degradation in torque, also shown in Fig. 11, can routinely be distinguished in dynamometer testing and for that reason is chosen as the criteria for advanced cavitation.

To mark this situation, we plot in Fig. 12, for each charge pressure, K-factor values against non-dimensional pump speed $\tilde{\Omega}_p$. In Fig. 12, line AD corresponds to 2% torque degradation. Thus advanced cavitation, depending on charge pressure values, occurs over a range of non-dimensional pump speeds $1.76 < \tilde{\Omega}_p < 2.01$. Therefore a conservative criteria for advanced cavitation, which is valid for the entire test matrix, is recommended to be $\tilde{\Omega}_p > 1.76$.

In our experiments, we also found that the peak strength of the cavity collapse zone is located closer to the pump inlet because the value of PS decreased for transducers located at increasing radial distance from the center of the pump (Fig. 4.23 in Zeng 2000).

CONCLUSIONS

Microwave telemetry and the identification of pressure fluctuation signals are able to infer the inception of cavitation in a torque converter before standard dynamometer testing.

Analysis in the frequency domain can separate, if needed, the effects of blade passage frequencies, and will allow various restrictions on the threshold values of frequency.

The Power Summation in the frequency domain provides a useful measure of cavitation signatures.

Non-dimensional pump speed can be directly and successfully used in practice to identify early cavitation for a range of charge pressures.

ACKNOWLEDGEMENTS

This research was sponsored by GM Powertrain, a division of the General Motors Corporation. The authors wish to express their gratitude to both Don Maddock of GM and Glen Barna of IR Telemetrics for technical support.

REFERENCES

Ardizzon, G., and Pavesi, G., 1994, "Numerical Prediction and Experimental Evaluation of Cavitation Inception on Centrifugal Pump Impellers," Cavitation and Gas-Liquid Flow in Fluid Machinery and Devices Proceedings, Vol. 190, ASME Fluids Engineering Division Summer Meeting.

Ceccio, S. L., and Brennen, C. E., 1992, "Dynamics of Attached Cavities on Bodies of Revolution," Journal of Fluids Engineering, Vol. 114, pp. 93 - 99, March.

Franz, R., Acosta, A. J., Brennen, C. E., and Caughey, T. K., 1990, "The Rotordynamic Forces on a Centrifugal Pump Impeller in the Presence of Cavitation," Journal of Fluids Engineering, Vol. 112.

Hashimoto, T., Yoshida, M., Watanabe, M., Kamijo, and K., Tsujimoto, Y., 1997, "Experimental Study on Rotating Cavitation of Rocket Propellant Pump Inducers," Journal of Propulsion and Power, Vol. 13, July-August.

Knapp, R. T., Daily, J. W., and Hammitt, F. G., 1970, Cavitation, McGraw-Hill, Inc., New York.

Kumar, S. and Brennen, C. E., 1993, "Some Nonlinear Interactive Effects in Bubbly Clouds," Journal of Fluid Mechanics, Vol. 225, pp. 565-591.

Maddock, D., 1991, "Application and Design of Automotive Torque Converters," Internal Monograph, GM Powertrain, General Motors Corporation, Ypsilanti, Michigan.

Munson, B. R., Young, D. F., and Okiishi, T. H., 1998, Fundamentals of Fluid Mechanics Third Edition, John Wiley & Sons, Inc.

Plesset, M. S., and Prosperetti, A., 1977, "Bubble Dynamics and Cavitation," Ann. Rev. Fluid Mech., Vol. 9, pp. 145- 185, March.

Rheingans W. J., and other authors, 1962, Symposium on Erosion and Cavitation, American Society for Testing and Materials, Philadelphia.

Tillner, W., Fritsch, H., Kruft, R., Lehmann, W., Louis, H., and Masendorf, G., edited by Barth, W. J., English translation edited by Turton, R. K., 1993, The Avoidance of Cavitation Damage, Mechanical Engineering Publications, London.

Zeng L., 2000, "Experimental Investigation of Cavitation Signatures in an Automotive Torque Converter," MSME Thesis, Michigan Technological University.

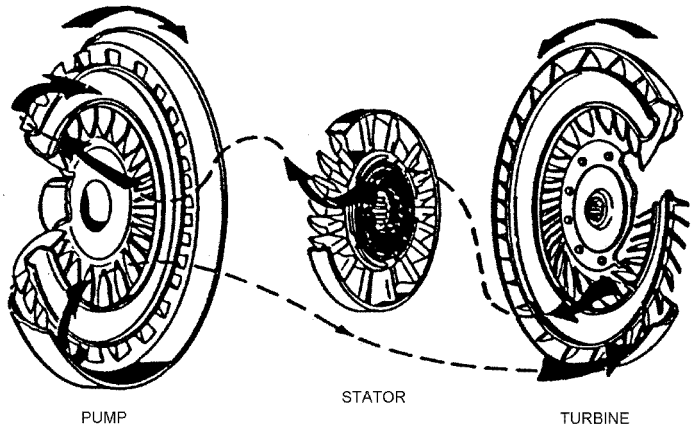

Figure 1. Components and working fluid flow path of a typical automotive torque converter.

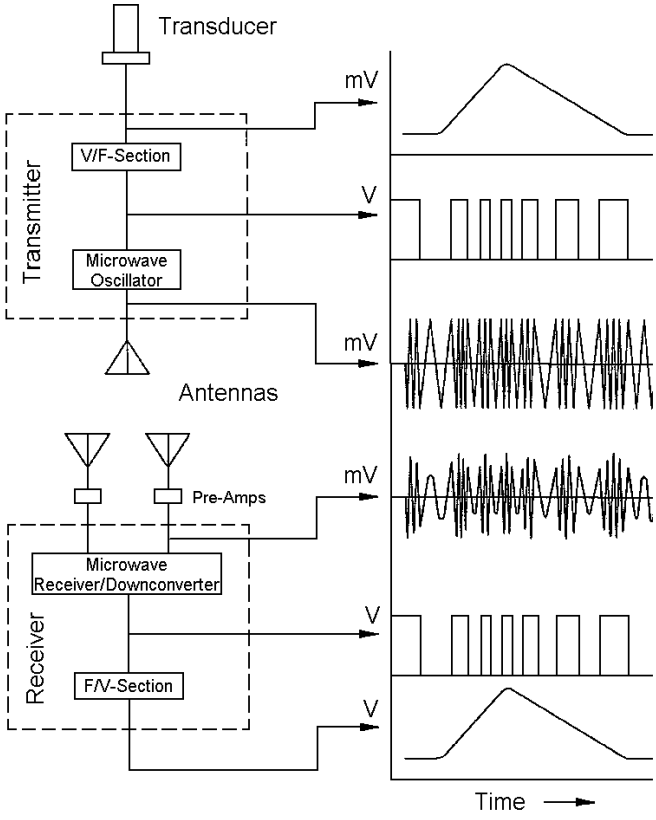

Figure 2. Evolution of the microwave telemetry signal.

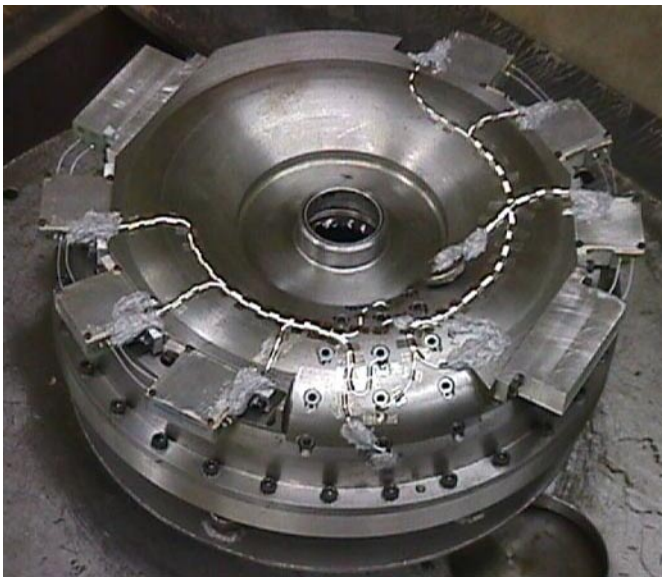

Figure 3. Telemetry packages mounted on the torque converter pump.

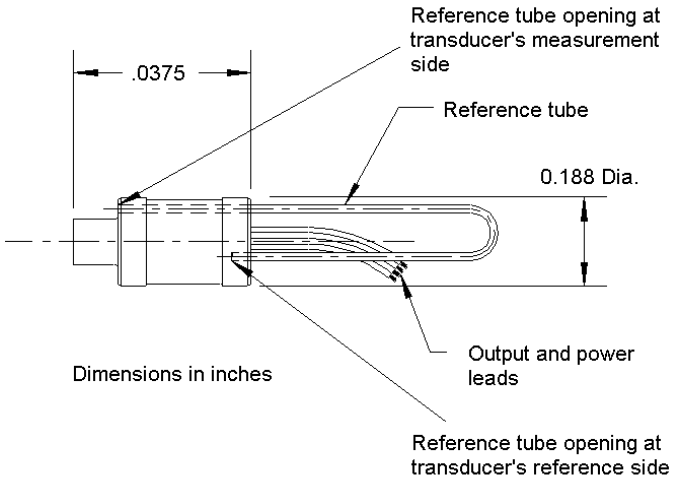

Figure 4. Differential pressure transducer used in torque converter experiment to measure *p'*.

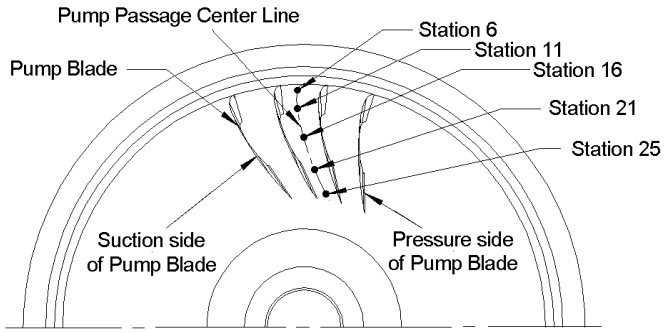

Figure 5. Radial locations of static pressure taps.

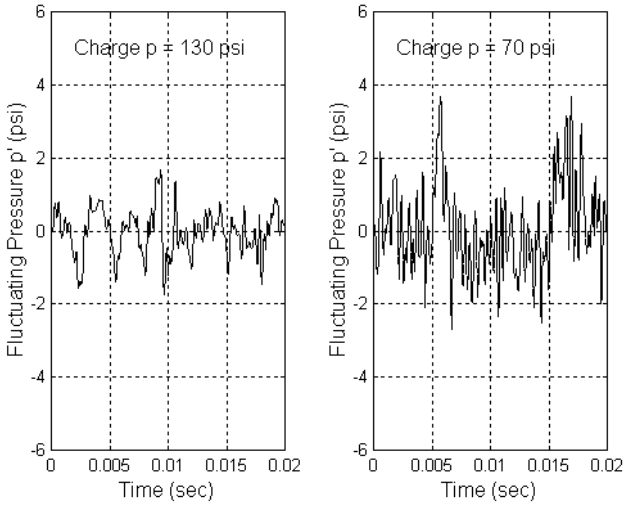

Figure 6. A representative pressure signal, *p'*, at station 25 and a pump speed of 1750 RPM .

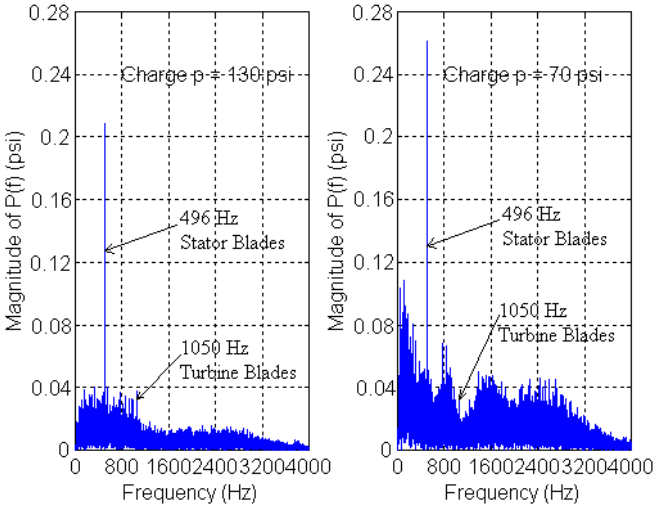

Figure 7. $|P(f)|$ values of data in Fig. 6.

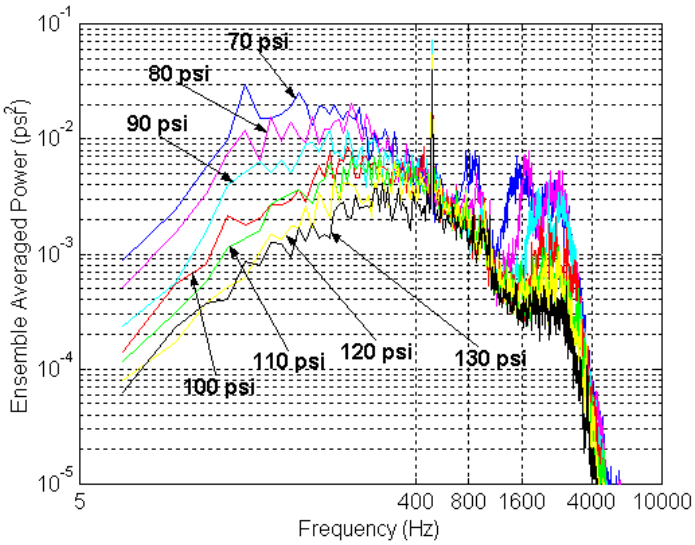

Figure 8. EAP (f) values for N=20, and various charge pressures at 1750 RPM.

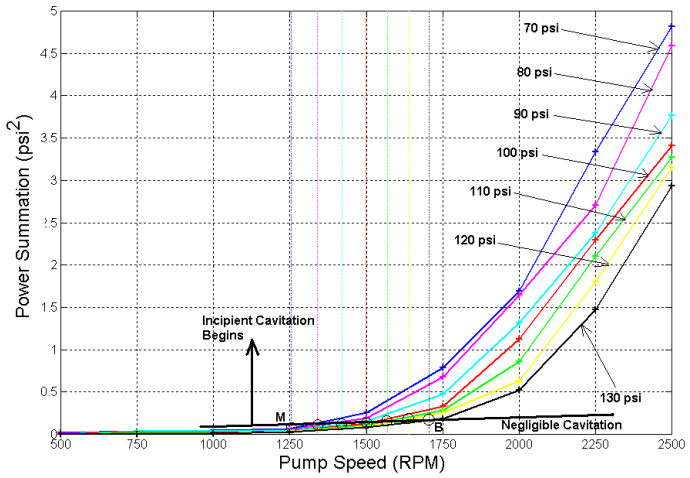

Figure 9. PS values as a function of pump speed and charge pressure.

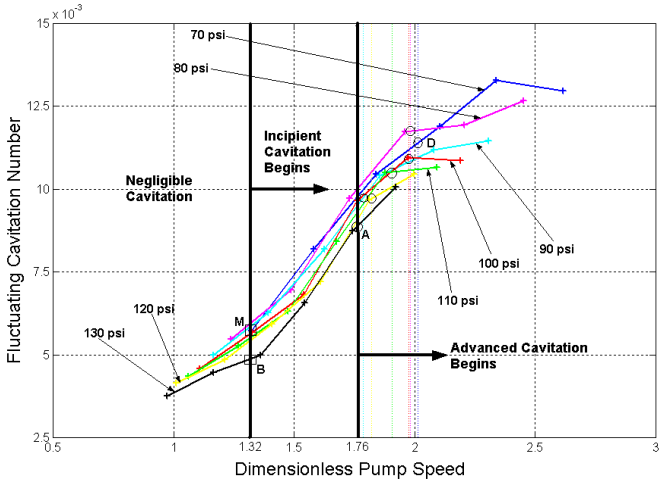

Figure 10. Fluctuating cavitation number, *Ca*', as a function of dimensionless pump speed at station 25.

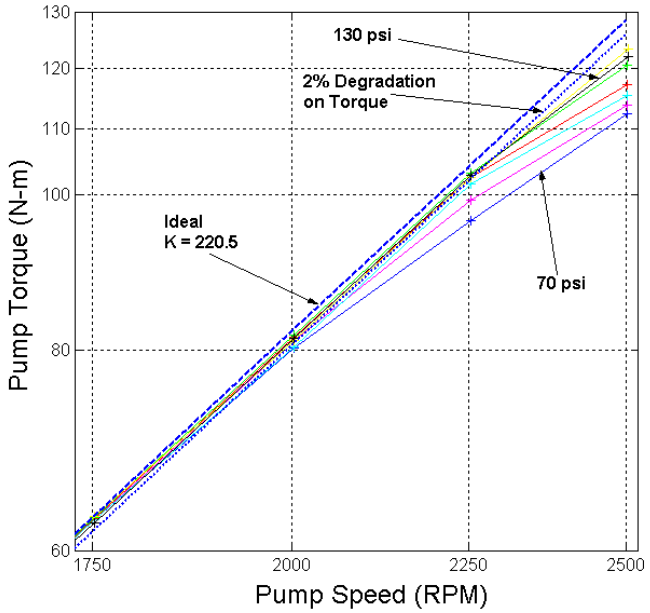

Figure 11. Pump torque as measured at the input shaft for various charge pressures.

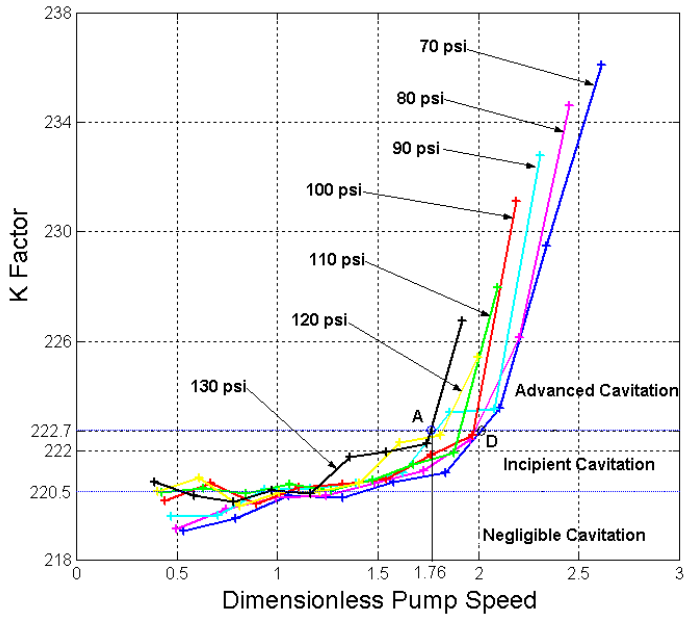

Figure 12. K-factor as a function of dimensionless pump speed at station 25.